PDK1–Akt pathway regulates radial neuronal migration and microtubules in the developing mouse neocortex

Yasuhiro Itoh[a,b,1,2], Maiko Higuchi[a,b], Koji Oishi[c], Yusuke Kishi[a,b], Tomohiko Okazaki[a,b], Hiroshi Sakai[a,b], Takaki Miyata[d], Kazunori Nakajima[c], and Yukiko Gotoh[a,b]

[a]Graduate School of Pharmaceutical Sciences, University of Tokyo, Tokyo 113-0033, Japan; [b]Institute of Molecular and Cellular Biosciences, University of Tokyo, Tokyo 113-0032, Japan; [c]Department of Anatomy, Keio University School of Medicine, Tokyo 160-8582, Japan; and [d]Department of Anatomy and Cell Biology, Nagoya University Graduate School of Medicine, Nagoya 466-8550, Japan

Edited by Pasko Rakic, Yale University, New Haven, CT, and approved April 15, 2016 (received for review August 19, 2015)

Neurons migrate a long radial distance by a process known as locomotion in the developing mammalian neocortex. During locomotion, immature neurons undergo saltatory movement along radial glia fibers. The molecular mechanisms that regulate the speed of locomotion are largely unknown. We now show that the serine/threonine kinase Akt and its activator phosphoinositide-dependent protein kinase 1 (PDK1) regulate the speed of locomotion of mouse neocortical neurons through the cortical plate. Inactivation of the PDK1–Akt pathway impaired the coordinated movement of the nucleus and centrosome, a microtubule-dependent process, during neuronal migration. Moreover, the PDK1–Akt pathway was found to control microtubules, likely by regulating the binding of accessory proteins including the dynactin subunit p150^{glued}. Consistent with this notion, we found that PDK1 regulates the expression of cytoplasmic dynein intermediate chain and light intermediate chain at a posttranscriptional level in the developing neocortex. Our results thus reveal an essential role for the PDK1–Akt pathway in the regulation of a key step of neuronal migration.

neuronal migration | neocortex | PDK1–Akt pathway | microtubule | dynein

In the developing mammalian neocortex, excitatory projection neurons born within the ventricular zone (VZ) migrate long distances radially toward the pia to form the six orderly aligned layers of the cortical plate (CP), thereby providing a basis for the establishment of functional neuronal connectivity (1). After neuronal fate commitment and delamination from the apical surface of the VZ, neurons first move into the subventricular zone (SVZ) and the intermediate zone (IZ), where they acquire a multipolar morphology. They then become bipolar and steer into the CP, through which they migrate by radial-glial–guided locomotion. As the neurons approach the pia, they switch their mode of migration to terminal somal translocation and settle down in the appropriate layer. There is a precise relation between the temporal order in which the various neuronal cell types are generated and their spatial distribution in the neocortex across mammalian species (2–5); abnormal neuronal migration underlies some human disorders of cortical development (6). Although various molecules and mechanisms have been implicated in regulating neuronal migration from its initiation to its termination (7–10), the mechanisms that regulate the speed of neuronal locomotion have remained unclear.

Locomotion is a unique mode of neuronal migration in which cells first stabilize and elongate their leading process. The centrosome then moves forward from the perinuclear region into the dilation/swelling of the leading process, followed by movement of the nucleus toward the centrosome and retraction of the cell rear. The cells then repeat this series of steps and move forward in a saltatory manner (8–10). Because centrosome–nucleus coupling is regulated by several genes that are mutated in human neurological diseases, the molecular mechanisms have been studied extensively. For example, Lis1, the product of a gene mutated in lissencephaly, and its associated proteins regulate pulling of the nucleus toward the centrosome by cytoplasmic dynein, a motor protein that directs transport toward the minus end of microtubules (8–10). The dynamic remodeling of microtubules is also important for neuronal migration (11, 12). Microtubule dynamics reflect a balance between the elongation and shortening of individual microtubules, and this balance is regulated by microtubule-associated proteins (MAPs) that either stabilize or destabilize microtubules (13, 14). Neuronal migration thus also depends on MAPs (8–10). Characterization of the mechanisms underlying the control of microtubule dynamics and the binding of MAPs to microtubules therefore is key to an understanding of neuronal migration and brain development. Moreover, the extracellular cues and intracellular signaling pathways that regulate microtubule dynamics in migrating neurons are not understood.

The serine/threonine kinase Akt (also known as protein kinase B) is phosphorylated and activated by phosphoinositide-dependent protein kinase 1 (PDK1) (15). The PDK1–Akt axis acts downstream of PI3K, which is activated by various extracellular stimuli, and it plays key roles in many biological processes, including microtubule stabilization, cell polarization, and cell migration (16–18). PI3K activity is required for normal radial migration in the neocortex (19, 20), but the contribution of the PDK1–Akt pathway to neuronal locomotion has remained elusive (20), possibly in part because of functional redundancy among the three Akt family members and the early death of Akt- and PDK1-mutant mice (21–23).

To examine the role of the PDK1–Akt pathway in neuronal migration, we have now determined the effects of conditional ablation of the PDK1 gene (*Pdpk1*) or inhibition of Akt with the

Significance

In the developing mammalian neocortex, neurons migrate a long distance from their birthplace to the positions where they form appropriate layers and networks, and dysregulation of this process has been implicated in brain malformation and neurological diseases. Given the fine correlation between temporal order of various sequentially generated neuronal cell types and their spatial distribution, migration speed needs to be tightly controlled to achieve correct neocortical layering, although the underlying mechanisms remain unclear. Here we show that the serine/threonine kinase Akt and its activator phosphoinositide-dependent protein kinase 1 (PDK1) regulate the speed of locomotion of mouse neocortical neurons through the cortical plate. Our data suggest that the PDK1–Akt axis regulates microtubule organization, in part by regulating the cytoplasmic dynein/dynactin complex, in migrating neurons.

Author contributions: Y.I. designed research; Y.I., M.H., Y.K., and T.O. performed research; T.M. and K.N. contributed new reagents/analytic tools; Y.I., M.H., K.O., and H.S. analyzed data; Y.G. supervised the study; and Y.I., M.H., and Y.G. wrote the paper.

The authors declare no conflict of interest.

This article is a PNAS Direct Submission.

[1]To whom correspondence should be addressed. Email: yasuhiro.m.itoh@gmail.com.

[2]Present address: Department of Stem Cell and Regenerative Biology, Harvard University, Cambridge, MA 02138.

This article contains supporting information online at www.pnas.org/lookup/suppl/doi:10.1073/pnas.1516321113/-/DCSupplemental.

use of in utero electroporation in the developing mouse CNS. We found that this pathway controls the speed of neuronal migration and the coordinated movement of the nucleus and centrosome during neuronal locomotion within the CP. Furthermore, our findings suggest that control of neuronal locomotion by the PDK1–Akt pathway is mediated at the level of microtubules, possibly through regulation of the cytoplasmic dynein/dynactin complex.

Results

Ablation of PDK1 Disrupts Neocortical Organization. To examine the role of PDK1 in neocortical development, we first crossed mice harboring a floxed *Pdpk1* allele (23) with those harboring a transgene for Cre recombinase under the control of a *Nestin* enhancer (24) to delete *Pdpk1* in neural progenitor cells (NPCs) and their descendants throughout the CNS. We previously showed that PDK1$^{flox/flox}$;Nestin-Cre mice die shortly after birth and have a reduced brain size (25). Immunohistofluorescence and immunoblot analyses confirmed that the abundance of PDK1 protein as well as the extent of Akt activation (as reflected by PDK1-mediated phosphorylation of Akt at Thr^{308} or phosphorylation of Akt substrates with a typical Akt phosphorylation consensus sequence) were markedly reduced in the brains of such mice at postnatal day (P) 0 (Fig. S1 *A*–*E* and *H*), indicating efficient ablation of PDK1.

We tested whether PDK1 regulates neocortical layering at P0 by immunostaining for Ctip2, a marker protein expressed at a high level in neurons of layer V and at a low level in those of layer VI, and for Cux1, a marker expressed in neurons of layers II–IV. The distribution of Ctip2$^+$ neurons was largely unchanged in PDK1$^{flox/flox}$;Nestin-Cre mice compared with control animals (Fig. 1 *A* and *B*). In contrast, Cux1$^+$ neurons were displaced from upper layers to deeper layers in the mutant brain (Fig. 1 *A* and *C*). These findings suggested that ablation of PDK1 resulted in malformation of the neocortex as manifested by a layering defect.

PDK1 Knockout Slows Radial Migration of Neocortical Neurons. Given that malformation of neocortical layers may result from defective neuronal migration, we examined whether radial migration of neurons is altered in the neocortex of PDK1$^{flox/flox}$;Nestin-Cre mice. We first performed birth dating analysis by injecting dams with BrdU at embryonic day (E) 15.5 and examining the neocortex at P0 (Fig. 1*D*). PDK1 mutation reduced the fraction of BrdU$^+$ cells in the CP and increased the fraction in the IZ, relative to control (Fig. 1 *D* and *E*), suggesting that PDK1 is required for the timely passage of migrating neurons from the IZ into the CP. Furthermore, the proportion of BrdU$^+$ cells in the upper region of the CP was significantly reduced in the mutant neocortex, even though the mutant brain is smaller. Thus these findings were consistent with the notion that PDK1 ablation slows the rate of radial neuronal migration.

To examine directly whether these changes in the distribution of BrdU$^+$ cells in the mutant neocortex were the result of slowed neuronal migration, we performed in utero electroporation at E15.5 with an expression plasmid for GFP and prepared brain slices at E18.5. Neuron locomotion in the CP was analyzed by time-lapse microscopy. Both control and mutant GFP$^+$ cells migrated radially toward the brain surface, rarely moving tangentially or backward (Fig. 1*G* and Movies S1 and S2). The average speed of locomotion of control GFP$^+$ cells was 21.1 ± 4.5 μm/h (mean ± SD), consistent with previous findings (26). However, mutant neurons migrated at the significantly reduced speed of 14.5 ± 3.9 μm/h (Fig. 1*H*). Importantly, we excluded rare dying cells from our analysis. These findings suggested that PDK1 is required for an appropriate speed of neuronal locomotion within the CP.

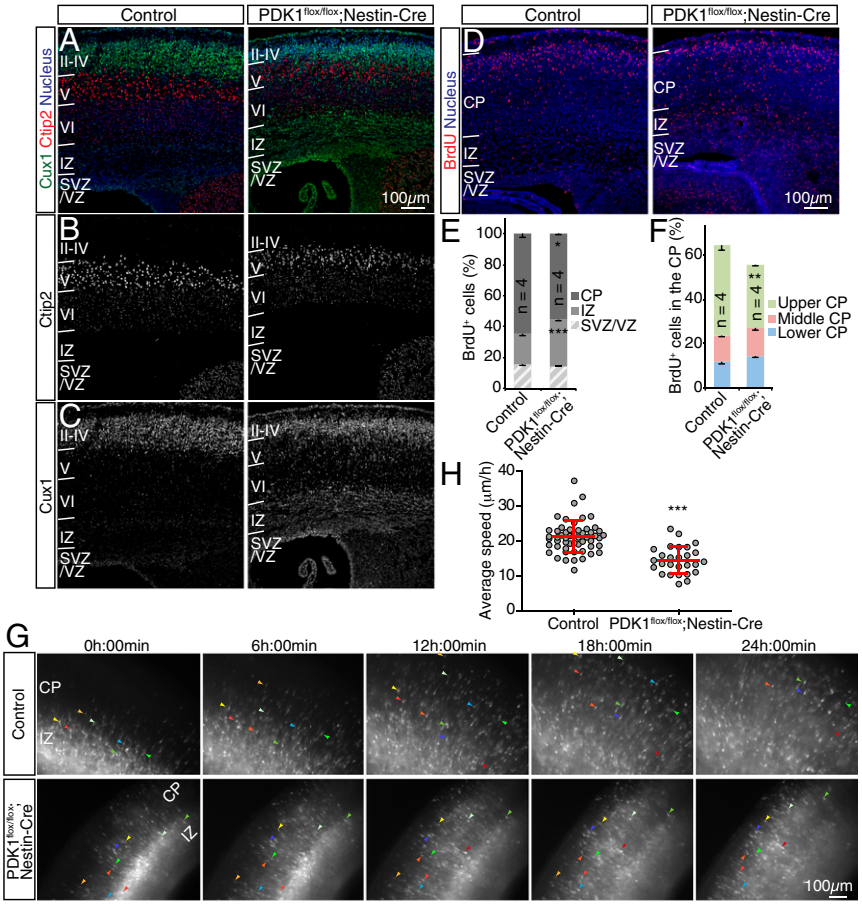

Fig. 1. Ablation of PDK1 slows radial neuronal migration in the developing mouse neocortex. (*A*–*C*) Coronal sections prepared from the brains of control or PDK1$^{flox/flox}$;Nestin-Cre mice at P0 were subjected to immunohistofluorescence staining with antibodies to the deep-layer and upper-layer markers Ctip2 (*A* and *B*) and Cux1 (*A* and *C*). Nuclei were stained with Hoechst 33342. (*D*–*F*) Coronal brain sections prepared at P0 from mice exposed to BrdU in utero at E15.5 were immunostained with antibodies to BrdU (*D*), and the distribution of BrdU$^+$ cells in the neocortical wall (*E*) or within the CP (*F*) was determined. Quantitative data are means ± SEM for the indicated number (*n*) of brains analyzed. (*G* and *H*) Cortical slices prepared at E18.5 from embryos subjected to in utero electroporation at E15.5 with a GFP expression plasmid were monitored for 24 h by fluorescence microscopy to follow the migration of GFP$^+$ cells (*G*). Colored arrowheads indicate the progress of individual neurons. (*H*) The average speed of radial migration was determined for individual neurons. Data are means ± SD for the 55 neurons examined for control slices and the 27 neurons examined for PDK1$^{flox/flox}$;Nestin-Cre slices. (Scale bars, 100 μm.) *P < 0.05, **P < 0.01, ***P < 0.001 (Student's t test) versus the corresponding control value.

Cell-Autonomous Regulation of Locomotion by PDK1. Neuronal migration is controlled by cell-autonomous as well as non–cell-autonomous mechanisms (8–10). Cell nonautonomous regulation includes the generation of Reelin-producing cells, formation and maintenance of a radial glial scaffold, and interaction with surrounding neurons. The distribution of Reelin$^+$ cells and the structure of both the radial glial scaffold and basal lamina appeared to be unchanged in the PDK1$^{flox/flox}$;Nestin-Cre neocortex, suggesting that PDK1 may be required cell autonomously (Fig. S1 *F* and *G*).

If PDK1 is required cell autonomously, then its knockout from postmitotic neurons should also alter lamination. We took advantage of Nex-Cre knockin mice, which express Cre recombinase in postmitotic neocortical pyramidal neurons, but not in NPCs or interneurons, under the control of the *Neurod6* promoter (27, 28). Immunohistofluorescence analysis revealed that although PDK1 was expressed uniformly within the CP of the control mouse neocortex at P1, its expression was attenuated in the superficial region of the CP in PDK1$^{flox/flox}$;Nex$^{Cre/+}$ mice (Fig. 2*A*). Consistent with this observation, phosphorylation of Akt at Thr^{308} and of Akt substrates was strongly reduced in the upper CP layers in the mutant (Fig. 2 *B* and *C*). These findings suggested that efficient ablation of PDK1 was achieved in neurons destined for the upper layers of the CP in the PDK1$^{flox/flox}$;Nex$^{Cre/+}$ neocortex. Because phosphorylation of Akt at Thr^{308} was attenuated throughout the neocortex and hippocampus of the mutant mice by P10 (Fig. S2*A*), PDK1 protein might be more stable in postmigratory than in migratory neurons in the developing neocortex, and a residual amount of PDK1 might be sufficient for Akt activation in cortical neurons of deeper layers at P1.

We next examined the layer structure of the neocortex. The distribution of deep-layer neurons as revealed by immunostaining for Ctip2 or for Tbr1, a marker of layer VI neurons, appeared unchanged in the brain of PDK1$^{flox/flox}$;Nex$^{Cre/+}$ mice at P1 (Fig. 2*D*). Most Cux1$^+$ upper-layer neurons had already reached the superficial region of the neocortex in both control and mutant mice by this time; in the mutant mice, however, the percentage of Cux1$^+$ cells was increased in the deep layers, although the total number of Cux1$^+$ cells was unchanged (Fig. 2 *E*–*G*). Neurons labeled with BrdU at E16.5 were also reduced in upper layers of the mutant neocortex as compared with the control (Fig. 2 *H*–*J*). Importantly, the fraction of Cux1$^+$ cells among BrdU$^+$ cells was similar in the two genotypes (Fig. 2*K*). Ectopic Cux1$^+$ neurons persisted in the deep layers until at least P10 (Fig. S2 *B* and *C*). These results suggested that upper-layer neurons of PDK1$^{flox/flox}$;Nex$^{Cre/+}$ mice are mispositioned.

To test whether the lower positioning of upper-layer neurons resulted from decreased migration, we measured the locomotion of mutant cells directly by time-lapse analysis. Neuronal locomotion within the CP was slowed in the mutant neocortex relative to control [control, 20.8 ± 4.9 μm/h; PDK1$^{flox/flox}$;Nex$^{Cre/+}$, 15.6 ± 5.0 μm/h (mean ± SD)] (Fig. 2*L* and Movies S3 and S4). Furthermore, PDK1 ablation in a small population of postmitotic neurons, achieved by in utero electroporation of the brain of PDK1$^{flox/flox}$ embryos with an expression plasmid for both GFP and Cre under the control of the *Neurod1* promoter, also was found to retard radial migration (Fig. S2 *D* and *E*), supporting the notion that PDK1 regulates the speed of neuronal locomotion through the CP during neocortical development in a cell-autonomous manner.

Akt Kinase Activity Regulates Radial Neuronal Migration. PDK1 phosphorylates and activates Akt and other members of the AGC protein kinase family (29). We focused on Akt in the present study

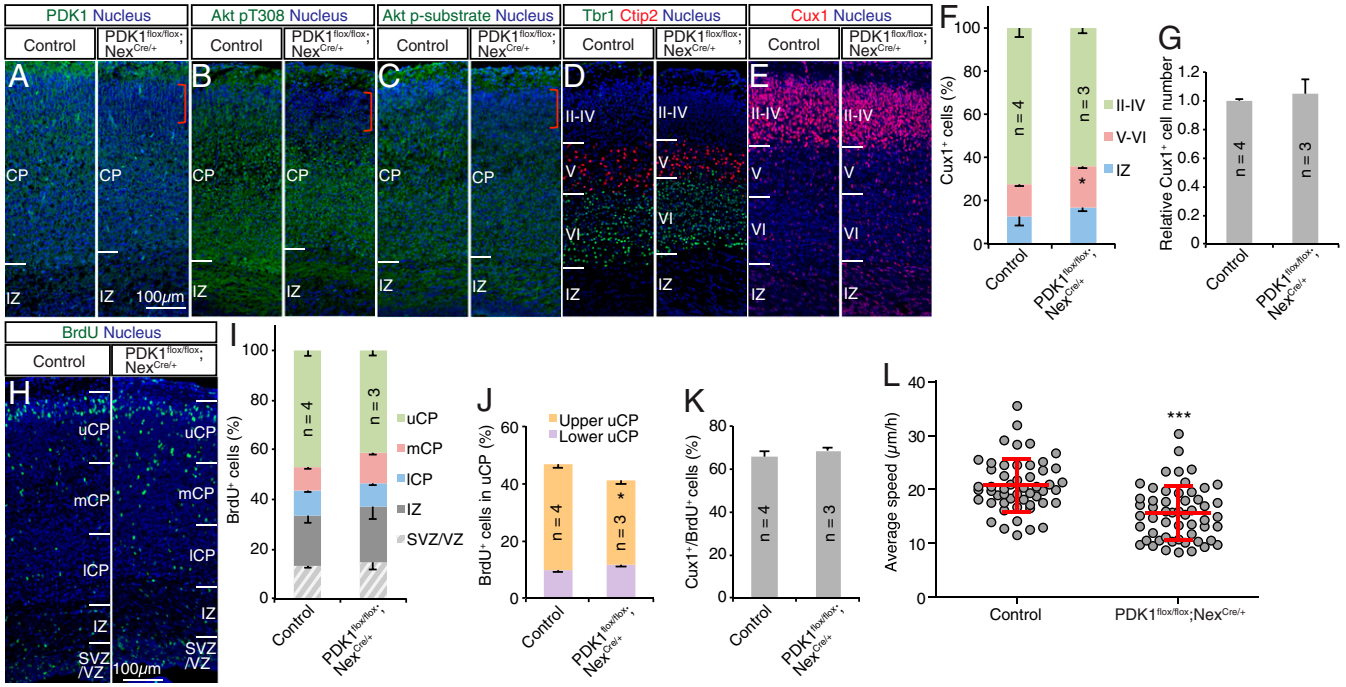

Fig. 2. PDK1 knockout in postmitotic neocortical neurons slows radial migration. (*A*–*G*) Coronal sections prepared from the brain of control or PDK1$^{flox/flox}$;Nex$^{Cre/+}$ mice at P1 were subjected to staining with antibodies to the indicated proteins and Hoechst 33342 (*A*–*E*). Red brackets in *A*–*C* indicate the superficial region of the CP where PDK1 is efficiently ablated in the mutant. (Scale bar, 100 μm.) (*F* and *G*) The distribution (*F*) and total number (*G*) of Cux1$^+$ cells were determined as means ± SEM for the indicated number (*n*) of brains analyzed. (*H*) Coronal brain sections prepared at P1 from mice exposed to BrdU in utero at E16.5 were stained with antibodies to BrdU and Hoechst 33342. (Scale bar, 100 μm.) uCP, mCP, and lCP denote upper, middle, and lower regions of the CP, respectively. (*I*–*K*) The distribution of BrdU$^+$ cells in the neocortical wall (*I*) or within the upper CP (*J*) and the proportion of Cux1$^+$ cells among BrdU$^+$ cells (*K*) were determined. Quantitative data are means ± SEM for the indicated number (*n*) of brains analyzed. (*L*) Cortical slices prepared at E18.5 from mouse embryos subjected to in utero electroporation at E15.5 with a GFP expression plasmid were monitored for up to 15 h by confocal microscopy to follow the migration of GFP$^+$ cells. The average speed of radial migration was determined for individual neurons. Data are means ± SD for the 52 neurons examined for control slices and the 54 neurons examined for PDK1$^{flox/flox}$;Nex$^{Cre/+}$ slices. *$P < 0.05$, ***$P < 0.001$ (Student's *t* test) versus the corresponding control value.

because of its role in nonneural cell migration (18). We examined whether Akt regulates radial neuronal migration by manipulating its kinase activity via in utero electroporation. To inhibit Akt kinase activity, we performed electroporation with an expression plasmid for both GFP and a kinase-inactive mutant of Akt1 (either K179A or K179A/T308A/S473A). Because both mutants were shown previously to function in a dominant-negative manner (16, 17) and yielded similar results in all experiments in the present study, we pooled the data obtained with the two constructs (together designated "Akt1 KN"). We also examined the effects of a constitutively active mutant of Akt1 (Akt mΔPH), in which the pleckstrin homology (PH) domain is replaced with a myristoylation sequence (30).

Most GFP$^+$ cells of control embryos transfected at E14.5 had migrated out of the VZ/SVZ and entered the CP by E17.5 and reached the superficial region of the CP by E18.5 (Fig. 3 *A*, *E*, *I*, and *K*–*O*). Although overexpression of Akt1 KN had little effect on GFP$^+$ cells at E16.5, by E17.5 and E18.5 there was a significant inhibition of migration to the upper CP, with a substantial increase in the number of cells remaining in the SVZ/VZ or IZ (Fig. 3 *B*, *F*, *J*, and *K*–*O*). These results suggested that Akt kinase activity is necessary for radial migration of neurons through the IZ and CP. Conversely, overexpression of Akt1 WT increased the proportion of GFP$^+$ cells reaching the superficial region of the CP and reduced the proportion of GFP$^+$ cells remaining in the IZ at E17.5, without having a significant effect at E16.5 (Fig. 3 *C*, *G*, and *K*–*M*). Because cells overexpressing Akt1 WT showed a moderately increased level of phosphorylation of Akt substrates (Fig. S3), an increase in Akt kinase activity appeared to promote the migration of neurons through the IZ and CP. In contrast, overexpression of constitutively active Akt mΔPH markedly abrogated the migration of neurons toward the brain surface, with GFP$^+$ cells apparently being stuck in the IZ and unable to enter the CP at E17.5 (Fig. 3 *D*, *H*, and *K*–*M*), possibly as a result of excessive or directionless activation of Akt (*Discussion*). Together, these findings suggested that Akt might play an important role in neuronal migration in a manner dependent on its kinase activity.

To examine whether Akt controls the speed of neuronal locomotion within the CP, we performed time-lapse analysis with cortical slices prepared at E16.5 or E17.5 from embryos subjected to in utero electroporation at E14.5 with expression plasmids for Akt1 WT or Akt1 KN, respectively. Although expression of Akt1 KN slowed radial migration [control, 21.1 ± 3.0 μm/h; Akt1 KN, 16.9 ± 3.2 μm/h (mean ± SD)] (Fig. 3*P*), overexpression of Akt1 WT increased migration speed [control, 19.7 ± 2.5 μm/h; Akt1 WT, 26.8 ± 7.6 μm/h (mean ± SD)] (Fig. 3*Q*). We rarely observed cells undergoing apoptosis or migrating tangentially or backward in the brains of embryos expressing either Akt1 KN or Akt1 WT. These results thus implicated Akt kinase activity in regulating the speed of neuronal locomotion through the CP in the developing neocortex.

Akt Kinase Activity in Postmitotic Neurons Regulates Radial Migration. We next investigated Akt function in neurons during radial migration by manipulating Akt kinase activity specifically in postmitotic neurons. Nex$^{Cre/+}$ embryos at E15.5 were subjected to in utero electroporation with plasmids constructed so that expression of the gene of interest is initiated by Cre-mediated excision of a stop sequence flanked by loxP sites (27, 31). The distribution of GFP$^+$ cells in fixed brain sections and the speed of radial migration within the CP of live brain slices were then determined.

Forced expression of Akt1 KN in postmitotic neurons reduced the speed of radial migration [control, 22.9 ± 4.0 μm/h; Akt1 KN, 16.2 ± 4.1 μm/h (mean ± SD)] (Fig. 4 *A*, *B*, and *E* and Movies S5 and S6). Conversely, overexpression of Akt1 WT in postmitotic

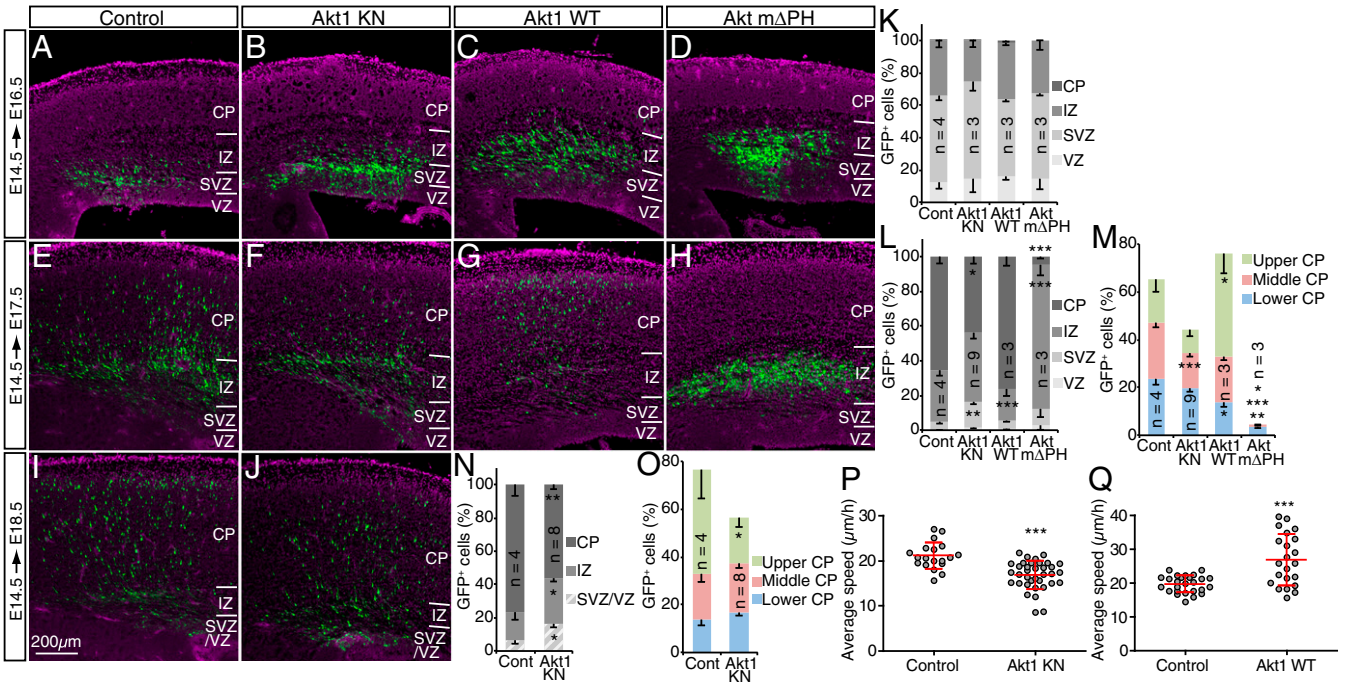

Fig. 3. Role of Akt kinase activity in radial neuronal migration. (*A*–*O*) The brains of embryos at E14.5 were subjected to in utero electroporation with expression plasmids for GFP alone (Control) (*A*, *E*, and *I*) or for GFP together with Akt1 KN (*B*, *F*, and *J*), Akt1 WT (*C* and *G*), or Akt mΔPH (*D* and *H*). GFP fluorescence (green) in coronal brain sections prepared at E16.5 (*A*–*D*), E17.5 (*E*–*H*), or E18.5 (*I* and *J*) was analyzed. Nuclei were stained with Hoechst 33342 (purple). (Scale bar, 200 μm.) The distribution of GFP$^+$ cells in the neocortex (*K*, *L*, and *N*) or within the CP (*M* and *O*) at E16.5 (*K*), E17.5 (*L* and *M*), or E18.5 (*N* and *O*) was determined. Data are means ± SEM for the indicated number (*n*) of brains analyzed. (*P* and *Q*) The brains of embryos at E14.5 were subjected to in utero electroporation with expression plasmids for GFP alone (Control) or for GFP together with either Akt1 KN (*P*) or Akt1 WT (*Q*). Cortical slices were prepared at E17.5 (*P*) or E16.5 (*Q*), and the migration of GFP$^+$ cells was monitored for 11 h 30 min. The average speed of radial migration was determined for individual neurons. Data are means ± SD for 19 neurons examined in control slices and 36 neurons examined in Akt1 KN slices (*P*), and for 26 neurons examined in control slices and 22 neurons examined in Akt1 WT slices (*Q*). $^*P < 0.05$, $^{**}P < 0.01$, $^{***}P < 0.001$ (Student's *t* test) versus the corresponding control value.

neurons increased migration speed [control, 21.7 ± 6.8 μm/h; Akt1 WT, 26.3 ± 8.0 μm/h (mean ± SD)] (Fig. 4 *C*, *D*, and *F* and Movies S7 and S8). Overexpression of either Akt1 KN or Akt1 WT in postmitotic neurons did not significantly affect the proportion of $Cux1^+$ cells among GFP^+ cells [normalized proportion of GFP^+ cells expressing Cux1: 1.0 ± 0.07 versus 0.77 ± 0.10 (means ± SEM) for control versus Akt1 KN, $P > 0.05$; 1.0 ± 0.11 versus 1.1 ± 0.10 for control versus Akt1 WT, $P > 0.05$]. Together, these results supported the notion that Akt kinase activity in neurons plays an important role in controlling the speed of neuronal locomotion through the CP in the developing neocortex.

We also examined whether glycogen synthase kinase 3 (GSK3), a key substrate of Akt, might play a role in neuronal migration. RNAi-mediated depletion of GSK3β perturbed radial migration in the embryonic neocortex (Fig. 5 *A*–*C*), consistent with previous observations (32). However, Akt-mediated phosphorylation of GSK3α at Ser^{21} or of GSK3β at Ser^9 may not be required for radial migration, given that migration was unaffected in GSK3 knockin mice in which these serine residues had been replaced by alanine (Fig. 5 *D*–*F*) (33). These results suggested that Akt and GSK3 regulate radial neuronal migration by independent mechanisms.

The PDK1–Akt Pathway Controls the Distance Between the Nucleus and Centrosome. We next asked which step (or steps) of locomotion is regulated by the PDK1–Akt pathway. The distance between the nucleus and centrosome in neurons migrating within the CP was measured by labeling the centrosome with DsRed fused to the centrosome-targeting domain of human pericentrin (Fig. 6*A*) (34). We focused on cells that had entered the CP but had not yet reached the pia. This analysis revealed that the position of the centrosome ranged from close to the nucleus to as far away as 15 μm from the nucleus in control brains, with the distribution of the distance similar to previous observations (Fig. 6*B*) (11). In $PDK1^{flox/flox}$;Nestin-Cre brains, however, this distance was reduced significantly (Fig. 6*B*). A similar shortening of the distance between the nucleus and centrosome was induced by forced expression of Akt1 KN (Fig. 6*C*). Although overexpression of Akt1 WT did not significantly affect this distance (Fig. 6*C*), it increased the proportion of migrating neurons in which the centrosome was positioned >7 μm away from the nucleus (control, 14.6%; Akt1 KN, 8.4%; Akt1 WT, 22.5%). We performed time-lapse analysis to observe time-dependent dynamics of the centrosome positioning. In both control and Akt1 KN-expressing neurons, the centrosome was located at the root of a leading process during most of the observation period. In control neurons, the centrosome repeatedly exhibited transient forward movement into the leading process, followed by forward movement of the cell body toward the centrosome (Fig. 6*D* and Movie S9). In neurons overexpressing Akt1 KN, however, the centrosome was less motile and remained in closer proximity to the cell body (Fig. 6*E* and Movie S10). We then measured the maximum distance between the centrosome and the cell body during the observation period and found that overexpression of Akt1 KN reduced that distance significantly (Fig. 6*F*). These results thus suggested that the PDK1–Akt pathway regulates the distance between the nucleus and centrosome, presumably through Akt kinase activity.

PDK1 Regulates Microtubules and MAP Binding to Microtubules. Because we found that the PDK1–Akt pathway controls nucleus–centrosome coupling, a process known to be dependent on microtubules (8–10), we hypothesized that this pathway might also regulate microtubule dynamics in cortical neurons. To examine this hypothesis, we separated polymerized microtubules from soluble tubulin in forebrain lysates of control and $PDK1^{flox/flox}$;Nestin-Cre mice at P0 by centrifugation and then compared the amount of polymerized microtubules in the pellet fraction. PDK1 ablation was found to reduce the amount of polymerized microtubules (Fig. 7*A*), suggesting that microtubules are less developed in the $PDK1^{flox/flox}$;Nestin-Cre brain.

We next investigated how PDK1 controls microtubules. Given that the binding of MAPs can affect the balance between elongation and shortening of microtubules and thereby the amount of polymerized microtubules (13, 14), we purified polymerized microtubules from the brains of control and $PDK1^{flox/flox}$;Nestin-Cre mice and then examined them for bound MAPs (Fig. S4). Although the binding of tau was reduced only marginally, the binding of MAP2a/b was attenuated markedly for microtubules prepared from the mutant brain (Fig. 7*B*). In addition, PDK1 knockout reduced the amount of microtubule-associated Lis1 and doublecortin (Dcx); the dysfunction of each of these proteins causes neuronal migration defects and brain malformation in both humans and mice (9). Furthermore, binding of the dynactin subunit $p150^{glued}$ and Ndel1, which together with Lis1 are regulators of dynein motor function (35), was reduced in microtubules prepared from the mutant brain (Fig. 7*B*). These findings suggested that the binding of MAPs to microtubules is widely disturbed by PDK1 ablation.

To observe microtubule structure and MAP distribution within neurons, we cultured cells isolated from the neocortex of control or $PDK1^{flox/flox}$;Nestin-Cre embryos at E15.5. Cells cultured for 3 or 4 d in vitro (DIV) were mostly positive for neuronal markers such as Dcx (Fig. S5). Control neurons manifested dense microtubule bundles along processes and mesh-like microtubule fibers surrounding the nucleus, as revealed by immunostaining for α-tubulin or tyrosinated α-tubulin, whereas mutant neurons exhibited thinner microtubule bundles in processes and fewer mesh-like microtubule fibers (Fig. 7*C* and Fig. S5*A*), suggesting that microtubules are less developed in PDK1-deficient cortical neurons. We also found that

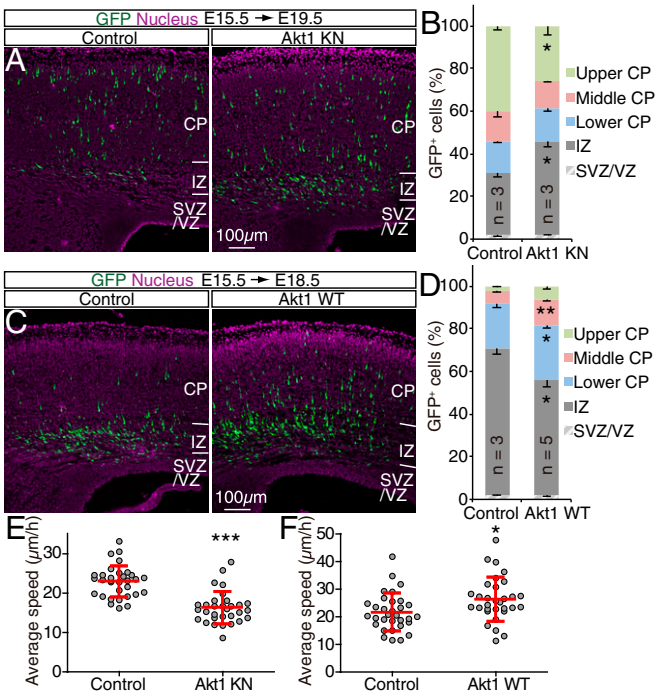

Fig. 4. Akt kinase activity in postmitotic neurons regulates radial migration. (*A*–*D*) The brains of $Nex^{Cre/+}$ embryos at E15.5 were subjected to in utero electroporation with Cre-dependent expression plasmids for GFP alone (Control) or for GFP together with Akt1 KN (*A*) or Akt1 WT (*C*). GFP fluorescence in coronal brain sections prepared at E19.5 (*A*) or E18.5 (*C*) was analyzed. Nuclei were stained with Hoechst 33342. (Scale bars, 100 μm.) The corresponding distributions of GFP^+ cells in the neocortex were determined as means ± SEM for the indicated number (*n*) of brains analyzed (*B* and *D*). (*E* and *F*) The brains of E15.5 $Nex^{Cre/+}$ embryos were subjected to in utero electroporation with Cre-dependent expression plasmids for GFP alone (Control) or for GFP together with Akt1 KN (*E*) or Akt1 WT (*F*), and cortical slices prepared at E18.5 were monitored for the migration of GFP^+ cells for up to 20 h. The average speed of radial migration was determined for individual neurons. Data are means ± SD for 31 or 32 neurons. $*P < 0.05$, $**P < 0.01$, $***P < 0.001$ (Student's *t* test) versus the corresponding control value.

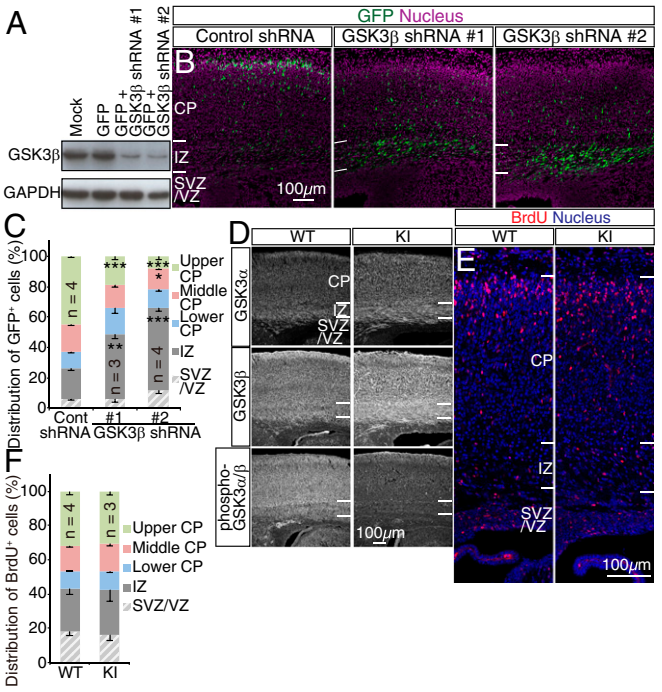

Fig. 5. Phosphorylation of GSK3 by Akt is dispensable for radial migration. (*A*) NIH 3T3 cells infected with retroviruses encoding GFP alone or GFP together with GSK3β shRNAs were subjected to immunoblot analysis with antibodies to GSK3β and to GAPDH (loading control). (*B*) GFP fluorescence in coronal brain sections prepared at E18.5 from embryos subjected to in utero electroporation at E14.5 with expression plasmids for both GFP and either GSK3β or control shRNAs was examined. (*C*) Nuclei were stained with Hoechst 33342. The distribution of GFP^+ cells in the neocortex was determined. Data are means ± SEM for the indicated number (*n*) of brains analyzed. (*D–F*) WT and $GSK3\alpha^{S21A/S21A}GSK3\beta^{S9A/S9A}$ (KI) embryos were exposed to BrdU in utero at E15.5 and fixed at E19.5/P0 for staining of coronal brain sections with antibodies to GSK3α, GSK3β, and phospho-GSK3α/β (*D*) or to BrdU and Hoechst 33342 (*E*). The distribution of $BrdU^+$ cells in the neocortex was determined (*F*). Data are means ± SEM for the indicated number (*n*) of brains analyzed. (Scale bars, 100 μm.) $^*P < 0.05$, $^{**}P < 0.01$, $^{***}P < 0.001$ (Student's *t* test) versus the corresponding control value.

the distribution of MAP2, Lis1, Ndel1, and $p150^{glued}$ was altered, but tau and Dcx were largely unaffected, in mutant neurons (Fig. S5 *B–G*). These results thus supported the notion that PDK1 regulates microtubule structure and MAP binding in cortical neurons.

Regulation of $p150^{glued}$ by Akt in Cortical Neurons. We previously showed that Akt regulates microtubules in fibroblasts (17), but the mechanism underlying this action of Akt has remained elusive. We therefore examined whether Akt might regulate MAPs in neurons. We subjected the neocortex of E14.5 embryos to in utero electroporation with an expression plasmid for GFP alone or GFP together with Akt1 KN or Akt1 WT, dissected the manipulated neocortical hemisphere at E15.5, dissociated the cells, and cultured them for 3 DIV. Overexpression of Akt1 KN did not appear to affect microtubule structure as visualized by immunostaining for α-tubulin or tyrosinated α-tubulin. The staining patterns of most of the MAPs we examined (tau, MAP2, Lis1, and Dcx) were also unchanged by Akt1 KN (Fig. S5 *H* and *I*). However, overexpression of Akt1 KN reduced, but overexpression of Akt1 WT increased, the intensity of the $p150^{glued}$ signal in the cell body (Fig. 7 *D* and *E*). These findings thus suggested that Akt contributes to the regulation of $p150^{glued}$ in neocortical neurons.

PDK1 Regulates the Expression of Cytoplasmic Dynein Subunits at a Posttranscriptional Level. The findings described above imply a regulation of the cytoplasmic dynein/dynactin complex by the PDK1–Akt pathway. We noticed that PDK1 knockout significantly reduces the levels of cytoplasmic dynein intermediate chain (DIC) and cytoplasmic dynein light intermediate chain (DLIC) proteins but not of $p150^{glued}$ in the P0 neocortex (Fig. 7*F*). Given that the levels of *Dync1i1* and *Dync1li1* mRNAs (encoding DIC and DLIC, respectively) were unchanged in the $PDK1^{flox/flox}$;Nestin-Cre neocortex (Fig. 7*G*), it is likely that PDK1 regulates the expression of DIC and DLIC at a posttranscriptional level. Taken together, our findings suggest that the PDK1–Akt pathway regulates neuronal migration, possibly by regulating the cytoplasmic dynein/dynactin complex.

Discussion

The PDK1–Akt pathway contributes to the regulation of proliferation, survival, differentiation of, and metabolism in various cell types (22, 25, 36), but its role in neuronal migration has been unclear. We demonstrated a role for the PDK1–Akt pathway in neocortical neurons through the specific manipulation of postmitotic cells with the use of $Nex^{Cre/+}$ mice or a *Neurod1* promoter–dependent Cre expression plasmid. Previous work suggested that Akt might be dispensable for neuronal locomotion (20). The discrepancy between our results and that earlier work (20) may be caused by differences in the experimental time course. Because PDK1–Akt inhibition slows down but does not arrest radial migration, the effects are most pronounced at short time courses. Our results obtained using in utero manipulation imply that the PDK1–Akt pathway is required cell autonomously, and no defects were observed in the radial glia or Reelin-producing cells. Furthermore, time-lapse imaging analysis of brain slices allowed us to assess the migration process directly. Mechanistic target of rapamycin (mTOR), a central regulator of cell metabolism and a downstream effector of Akt, appears unlikely to mediate the action of the PDK1–Akt pathway during radial migration, because rapamycin treatment or knockout of mTOR in postmitotic cortical neurons was shown not to affect radial migration (37, 38). Although, in theory, decreased cell survival might contribute to decreased neuronal migration or brain malformation, the migration increase by Akt1 WT overexpression is presumably unrelated to cell survival. Moreover, we found that the PDK1–Akt pathway controls coupling of the nucleus and the centrosome via regulation of microtubules. Because PI3K is implicated in regulating the tangential migration of interneurons derived from the medial ganglionic eminence (39), the PDK1–Akt pathway might have a conserved role in neuronal migration across CNS regions and neuronal subtypes.

An intriguing finding of our study is that Akt kinase activity is important for setting the speed of neurons during bipolar locomotion. Neocortical neurons move discontinuously and change their speed relatively frequently (26, 40), suggesting that they may be equipped with mechanisms that allow them to adjust their radial migration in response to changes in the extracellular environment. In this regard, growth factor stimulation triggers transient Akt activation, which decays within 10–30 min depending on the stimulus and cell type (16, 41). Thus it is possible that Akt activity modulates the speed of neuronal locomotion in response to the extracellular environment.

In addition to temporal regulation, spatial regulation of Akt kinase activity is an important factor in radial neuronal migration. Overexpression of Akt1 WT enhanced radial migration, whereas overexpression of a constitutively active Akt1 mutant (Akt mΔPH) impaired radial migration. Given that Akt is activated locally as a result of its translocation to the plasma membrane triggered by the PI3K-mediated generation of phosphatidylinositol 3,4,5-trisphosphate (PIP_3), overexpression of Akt1 WT may have sensitized neurons to unknown extracellular cues that induce the production of PIP_3. On the other hand, Akt mΔPH is activated at the plasma membrane independently of PIP_3 and without directionality as a result of the replacement of the PH domain with a myristoylation sequence. We therefore propose that correct activation of Akt is important for neuronal migration. Forced expression of Akt mΔPH also induced a marked accumulation of multipolar cells in the IZ

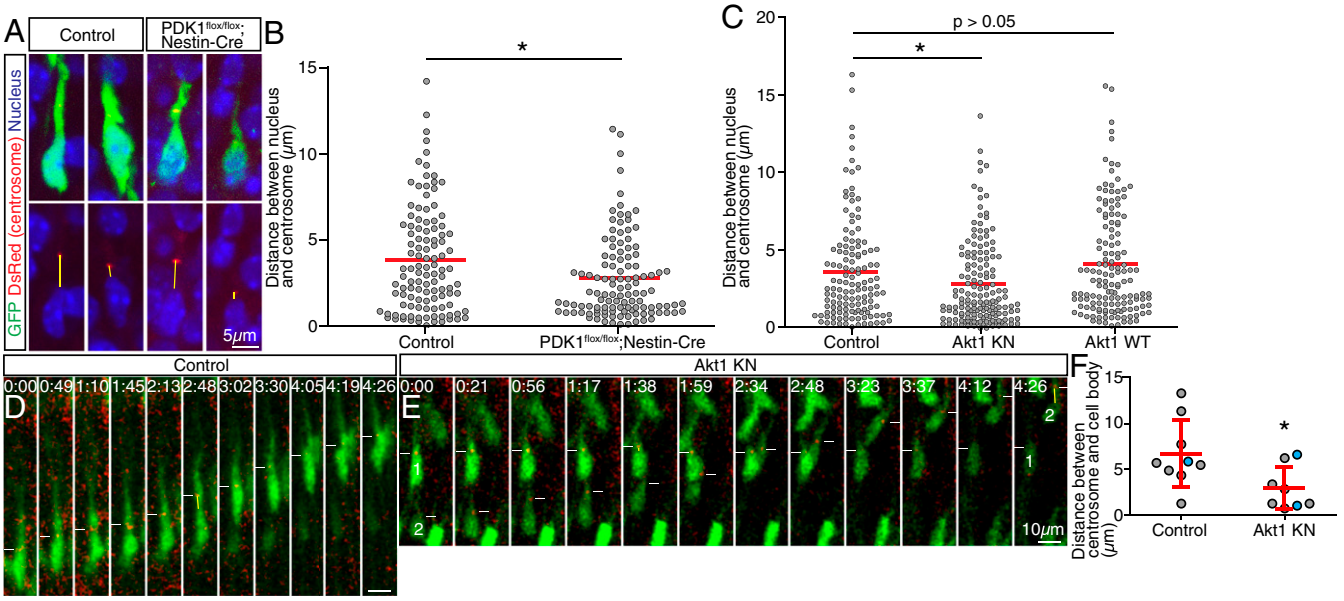

Fig. 6. Coordinated movement of the nucleus and centrosome is controlled by the PDK1–Akt pathway. (*A*) Control or PDK1$^{flox/flox}$;Nestin-Cre embryos at E15.5 were infected in utero with retroviruses encoding both GFP and a fusion construct of DsRed and the centrosome-targeting domain of human pericentrin. Neurons migrating within the CP of the neocortex at P0 were examined for intrinsic DsRed fluorescence and for GFP immunofluorescence. Nuclei were stained with TO-PRO3. Yellow lines indicate the distance between the nucleus and centrosome. (Scale bar, 5 μm.) (*B*) The distribution of this distance was determined. The red lines indicate mean values for 112 neurons in control brains and 115 neurons in PDK1$^{flox/flox}$;Nestin-Cre brains. *$P < 0.05$ (Mann–Whitney test). (*C*) Analysis of the distance between the nucleus and centrosome in neocortical neurons migrating within the CP at E18.5 after in utero electroporation at E14.5 with expression plasmids for GFP and centrosome-targeted DsRed either alone (Control) or together with Akt1 KN or Akt1 WT. Red lines indicate mean values for 130, 154, and 142 neurons, respectively. *$P < 0.05$ (Mann–Whitney test). (*D* and *E*) Cortical slices prepared at E17.5 from embryos subjected to in utero electroporation at E14.5 with expression plasmids for GFP (green) and centrosome-targeted DsRed (red) either alone (Control) (*D*) or together with Akt1 KN (*E*) were monitored for 4.5 h. White lines indicate the level of centrosome location. (Scale bar, 10 μm.) (*F*) The maximum distance between the centrosome and cell body during observation (indicated by yellow lines) was determined for individual neurons. Data shown in blue are from neurons shown in *D* and *E*. Data are means ± SD for the nine neurons examined for control and the eight neurons examined for Akt1 KN. *$P < 0.05$ (Student's *t* test).

(Fig. 3), suggesting that polarized Akt activation also might contribute to specification of the leading process (42).

The PDK1–Akt pathway is activated by various extracellular factors. Ligands and receptors upstream of this pathway are not addressed in our study. However, TrkB is a candidate receptor for regulation of the PDK1–Akt axis during neuronal migration, because TrkB is localized along the leading process of migrating interneurons derived from the medial ganglionic eminence, TrkB stimulation by BDNF activates Akt in cortical neurons, and cortical neuronal migration is delayed by knockdown or knockout of TrkB or by knockin mutation of TrkB intracellular residues critical for Akt activation (39, 43, 44). The proneural transcription factor NeuroD1 was recently shown to up-regulate TrkB expression (45), suggesting that cortical cells may gain responsiveness to TrkB ligands (such as BDNF) on commitment to the neuronal fate. In addition, the extracellular matrix component laminin γ1 and its integrin receptor might function upstream of the PDK1–Akt pathway during neuronal migration (46). Furthermore, given that *N*-cadherin mediates neuron–glial cell adhesion and regulates Akt activation (36, 47), Akt might be activated at sites of such adhesion in an *N*-cadherin–dependent manner. Although previous work suggested that Akt might function downstream of Reelin during cortical development (38), PDK1 ablation resulted in a layering defect distinct from that of *reeler* mutants, suggesting that Akt is not a central effector of Reelin signaling, at least during radial neuronal migration.

Akt is required to localize the growing microtubule plus end-tracking protein EB1 to the embryonic cell cortex in the *Drosophila* early embryo (48). Furthermore, cytoplasmic dynein tracks the growing microtubule plus end via p150^{glued} in an EB1-dependent manner (49). The PDK1–Akt pathway therefore might have a conserved role in regulating microtubule organization, possibly through an action at the microtubule plus end, across cell types with distinct morphologies.

We identified the cytoplasmic dynein/dynactin complex as a potential Akt effector in the regulation of radial migration. Dynein is concentrated both at the dilation/swelling of the leading process and in the soma of neocortical neurons. Dynein at the dilation/swelling has been proposed to pull the microtubule network and the centrosome, whereas dynein at the nuclear surface is thought to contribute to the forward movement of the nucleus by transmitting force to this organelle (11). Because we found that inhibition or activation of the PDK1–Akt pathway shortens and activation of the PDK1–Akt pathway lengthens the distance between the nucleus and centrosome, we hypothesize that activation of PDK1–Akt signaling facilitates dynein motor activation in the leading process and around the dilation/swelling, thereby triggering forward movement of the centrosome. Our study revealed that PDK1 regulates the expression of cytoplasmic dynein subunits at a posttranscriptional level, and we predict that the reduction in the binding of p150^{glued} to polymerized microtubules in the PDK1-null brain or the reduction in the amount of somal p150^{glued} by inhibition of Akt activity could be attributed, at least in part, to the reduced expression of cytoplasmic dynein subunits. As far as we are aware, mechanisms controlling the levels of cytoplasmic dynein subunits in mammalian cells are not well understood, with the exception that NudC-like protein contributes to the stabilization of the DIC (50); therefore in future studies it would be interesting to investigate the molecular mechanism by which the PDK1–Akt pathway regulates cytoplasmic dynein/dynactin complex.

We showed that the PDK1–Akt pathway controls the speed of radially migrating neurons, but inhibition or activation of this pathway changed the speed by only 20–30%, an effect that might not be considered substantial. Indeed, deep-layer neurons were positioned normally at birth. In contrast, upper-layer neurons have not reached their normal positions at birth, suggesting that neurons migrating longer distances are more vulnerable to changes in

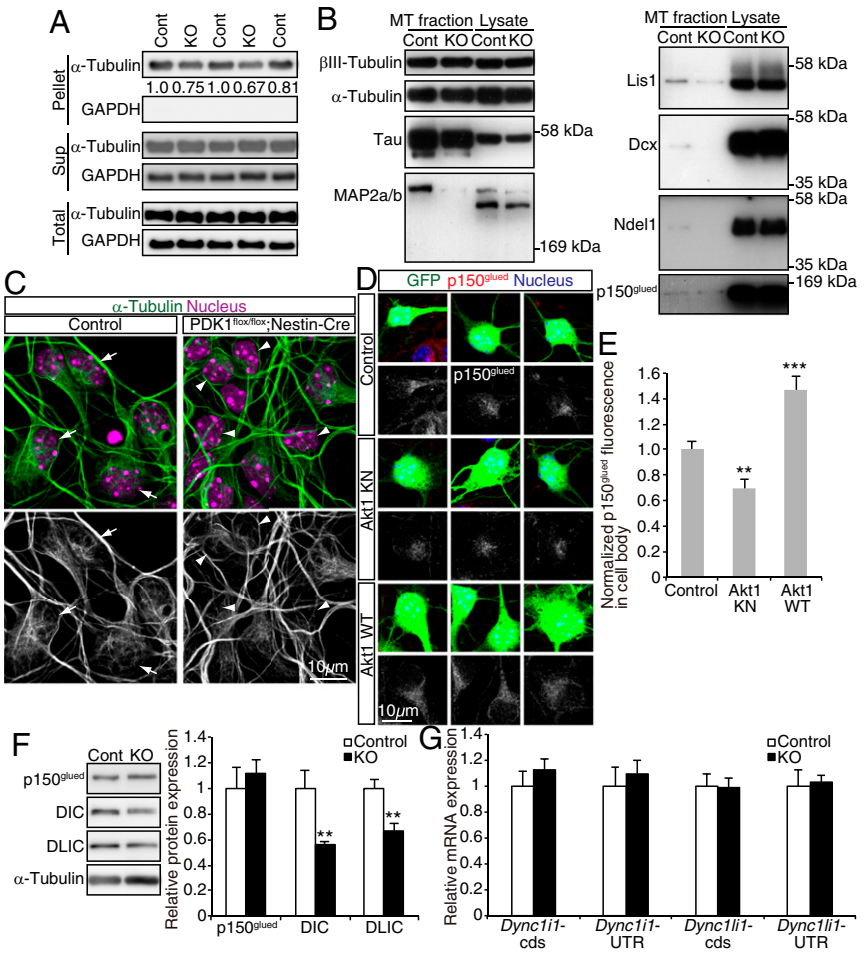

Fig. 7. The PDK1–Akt pathway regulates microtubules in cortical neurons. (*A*) Fractionation of soluble (Sup, monomer) and insoluble (Pellet, polymer) tubulin by centrifugation of forebrain lysates prepared from control (Cont) or PDK1$^{flox/flox}$;Nestin-Cre (KO) mice at P0. The total, soluble, and insoluble fractions were subjected to immunoblot analysis with antibodies to α-tubulin and GAPDH (as a loading control). The amount of insoluble α-tubulin normalized by the amount of total α-tubulin is expressed in arbitrary units. Each lane corresponds to one animal. (*B*) Polymerized microtubules (MT fraction) purified from E19.5 control or PDK1$^{flox/flox}$;Nestin-Cre mouse brain homogenates and the total homogenates (Lysate) were subjected to immunoblot analysis with antibodies to the indicated proteins. Similar results were obtained for six animals of each genotype in two independent experiments. (*C*) Primary neurons isolated from the E15.5 neocortex were cultured for 3 or 4 DIV and then were stained with antibodies to α-tubulin and Hoechst 33342. Arrows indicate representative cells with a mesh-like microtubule structure; arrowheads indicate cells with a less elaborate microtubule structure around the nucleus. (Scale bar, 10 μm.) Similar results were obtained for five control embryos and four PDK1$^{flox/flox}$;Nestin-Cre embryos. (*D*) Primary neurons were isolated from the E15.5 neocortex of embryos subjected to in utero electroporation at E14.5 with expression plasmids for GFP alone (Control) or for GFP together with Akt1 KN or Akt1 WT. The neurons were cultured for 3 DIV and then were stained with antibodies to p150^{glued} and Hoechst 33342. (Scale bar, 10 μm.) (*E*) The intensity of p150^{glued} immunofluorescence within the cell body of GFP^{+} cells was measured. Data are means ± SEM for 28, 20, and 25 cells (from three or four brains) for control, Akt1 KN, and Akt1 WT, respectively. (*F* and *G*) Expression of p150^{glued}, DIC (*Dync1i1*), or DLIC (*Dync1li1*) at the protein and mRNA levels in P0 control (Cont) or PDK1$^{flox/flox}$;Nestin-Cre (KO) neocortex analyzed by immunoblotting (*F*) or quantitative RT-PCR (*G*). Expression levels of protein or mRNA were normalized to that of α-tubulin or β-actin (*Actb*), respectively. Data are means ± SD from three animals. $^{**}P < 0.01$, $^{***}P < 0.001$ (Student's *t* test).

migration speed. Regulation of the speed of neuronal migration therefore is likely to be of greater relevance in thicker cortical regions, such as the frontal cortex, and in organisms with larger brains, such as humans. A slowing of neuronal migration may result in premature cessation of locomotion as a consequence of the disappearance of the glial scaffold caused by the terminal differentiation of radial glia into neurons or astrocytes. Dysregulated Akt signaling has been associated with neurological conditions such as autism spectrum disorders and focal cortical dysplasia (51, 52), and *AKT1* is a candidate susceptibility gene for schizophrenia (53). An altered speed of radial neuronal migration and resultant layer malformation may contribute, at least in part, to the pathogenesis of these psychiatric disorders.

Materials and Methods

Animals. *Pdpk1*$^{flox/flox}$ (PDK1$^{flox/flox}$), Nestin-Cre, Nex-Cre, and GSK3α$^{S21A/S21A}$ GSK3β$^{S9A/S9A}$ mice with a C57BL/6J background were described previously (23–25, 27, 33). C57BL/6J and pregnant ICR mice were obtained from Oriental Yeast Co. and CLEA Japan, respectively. E1 was defined as 12 h after detection of a vaginal plug. Dams were injected i.p. with BrdU (50 mg/kg) diluted in PBS. All mice were maintained and treated in accordance with protocols approved by the Animal Care and Use Committee of the University of Tokyo.

PDK1$^{flox/flox}$;Nestin-Cre mice die shortly after birth (25), whereas PDK1$^{flox/+}$;Nestin-Cre mice grow normally and are fertile. The brains of PDK1$^{flox/+}$;Nestin-Cre mice appeared indistinguishable from those of PDK1$^{flox/+}$ or PDK1$^{flox/flox}$ mice in our analyses, and we therefore pooled data from the brains of these genotypes as controls (unless indicated otherwise). PDK1$^{flox/flox}$;Nex$^{Cre/+}$ mice are viable and survive to adulthood, but they grow poorly and are sterile. PDK1$^{flox/+}$;Nex$^{Cre/+}$ mice grow normally and are fertile. We crossed PDK1$^{flox/+}$;Nex$^{Cre/Cre}$ male mice, which also grow normally and are fertile, with PDK1$^{flox/flox}$ or PDK1$^{flox/+}$ females to obtain control and PDK1$^{flox/flox}$;Nex$^{Cre/+}$ animals. The brains of PDK1$^{flox/+}$Nex$^{Cre/+}$ mice appeared indistinguishable from those of PDK1$^{+/+}$Nex$^{Cre/+}$ mice in our analyses; therefore we pooled data from the brains of these genotypes as controls.

Plasmid Constructs and RNAi. cDNAs encoding constitutively active Akt1 [Akt mΔPH, in which the PH domain (residues 4–129) of human Akt1 is replaced with a myristoylation site at the NH_2 terminus] and kinase-inactive human Akt1 (Akt1 KA; K179A) were kindly provided by R. Roth, Stanford University, Stanford, CA, and D. R. Alessi, University of Dundee, Dundee, UK, respectively. Akt1 3A (K179A/T308A/S473A) was described previously (54). The cDNAs encoding wild-type or mutant Akt1 were inserted into the expression vectors pCAG-IRES-GFP or pCAG-floxpA. The plasmids pCAG-floxpA and pCAG-floxpA-EGFP were kindly provided by F. Matsuzaki, RIKEN CDB, Kobe, Japan (31). A cDNA for Cre recombinase was inserted into pCAGEN or pNeuroD1-IRES-GFP. pCAG-IRES-GFP and pCAGEN were kindly provided by C. L. Cepko, Harvard Medical School, Boston, and T. Matsuda, Kyoto University, Kyoto (55), and pNeuroD1-IRES-GFP was kindly provided by F. Polleux, Columbia University, New York (42). An expression plasmid for DsRed fused to the centrosome-targeting domain of human pericentrin was kindly provided by S. Munro, MRC Laboratory of Molecular Biology, Cambridge, UK (34), and cDNA encoding the DsRed-pericentrin fusion protein was cloned into pMXs-IRES-GFP (56).

For construction of GSK3β shRNA vectors, oligonucleotides corresponding to the target coding sequence and the complementary sequence were inserted into the pSIREN vector (BD Biosciences) (57). The targeting sequences were as follows: GSK3β shRNA no. 1, 5′-GACGCTCCCTGTGATCTATGT-3′; GSK3β shRNA no. 2, 5′-GTTCTACAGGACAAGCGATTT-3′; and control shRNA, 5′-GACGTCTAACGGATTCGAGCT-3′.

In Utero Electroporation or Retroviral Infection and Slice Culture. Introduction of plasmid DNA or retroviruses into neuroepithelial cells of the developing

mouse neocortex was performed as previously described (58, 59). In brief, plasmid DNA or retroviruses (1 μL) were injected into the lateral ventricle of embryos at the indicated developmental stages. pCAG-IRES-GFP, pCAGEN, and pSIREN plasmids were injected at 2 μg/μL, and pCAG-floxpA constructs were injected at 1–8 μg/μL. DsRed-pericentrin or pNeuroD1 constructs were injected at 0.5 or 4 μg/μL, respectively. For electroporation, electrodes were positioned at the flanking ventricular regions of each embryo, and four or five 50-ms pulses of 35 V were applied at intervals of 950 ms with an electroporator (CUY21E; Tokiwa Science). The embryos were isolated after the indicated number of days for immunohistofluorescence analysis of the brain.

For live imaging of migrating neurons, brain slices were prepared 2 or 3 d after electroporation. The brain was removed rapidly, and coronal slices (300 μm) were prepared with a vibratome (LinearSlicer PRO7; Dosaka EM) and maintained on Millicell inserts (EMD Millipore) in Neurobasal medium (Gibco) supplemented with 2% B27 (Invitrogen) and 2 mM glutamate. Time-lapse images were captured every 10–30 min for 6–24 h for low-magnification images (10× objective) or every 7 min for 4.5 h for high-magnification images (40× objective, long distance) with the use of a confocal (Leica SP5) or epifluorescence (Nikon) microscope, each equipped with an incubation chamber (37 °C, 5% CO_2, humidified). Neurons migrating within the CP were analyzed with the use of TCS-SP5 (Leica), Slide Book (Nippon Roper), or ImageJ software. Gaussian blur filtering (pixel radius = 1) was applied to time-lapse images taken with 40× objective lens.

Immunohistofluorescence Analysis. Immunohistofluorescence analysis was performed as previously described (58). For BrdU or PDK1 staining, sections were autoclaved in target retrieval solution (DAKO) or in 10 mM sodium citrate buffer (pH 6.0) at 105 °C for 5 min. Images were acquired with an LSM510 (Zeiss) or TCS-SP5 (Leica) confocal microscope and were processed with Photoshop CS software (Adobe). The boundaries between the VZ and the SVZ, between the SVZ and the IZ, and between the IZ and the CP were determined by the orientation and density of counterstained nuclei. The distance between the centrosome and nucleus was measured with the use of LSM510 or TCS-SP5 software.

Antibodies. Primary antibodies for immunostaining or immunoblot analysis included mouse monoclonal antibodies to BrdU (BD Biosciences, 347580, 1:200 dilution), to PDK1 (Santa Cruz, E-3, 1:500 for immunoblot analysis), to Akt pS473 [Cell Signaling Technology (CST), 4051, 587F11, 1:200 for immunostaining], to α-tubulin (Sigma, T6199, 1:1,000), to βIII-tubulin (Covance, MMS-435P, 1:1,000), to GAPDH (Millipore, MAB374, 1:2,000), to tau (Chemicon, MAB3420, 1:1,000), to MAP2a/b (Sigma, M1406, AP-20, 1:1,000), to MAP2a/b/c (Sigma, M4403, HM-2, 1:1,000), to Lis1 (Sigma, L7391, 1:500 for immunoblot analysis and 1:200 for immunostaining), to $p150^{glued}$ (BD Biosciences, 610473, 1:300–1:500), to Nestin (BD Biosciences, 556309, 1:200), to Reelin (CR-50, 1:2,000) (60), to DIC (Abcam, ab23905, 1:1,000), and to GSK3β (BD Biosciences, 610201, 1:1,000 for immunoblot analysis and 1:500 for immunostaining); goat polyclonal antibodies to Dcx (Santa Cruz, sc8066, 1:200); rat monoclonal antibodies to Ctip2 (Abcam, ab18465, 1:2,000) and to tyrosinated α-tubulin (Millipore, MAB1864, YL1/2, 1:500); rabbit polyclonal antibodies to GFP (MBL International, 598, 1:1,000), to Cux1 (Santa Cruz, sc13024, 1:200), to PDK1 (Abcam, ab31406, 1:200 for immunostaining), to Akt pT308 (Santa Cruz, sc16646, 1:300 for immunoblot analysis), to Akt pS473 (CST, 9271, 1:1,000 for immunoblot analysis), to phospho-GSK3α/β (CST, 9331, 1:200), to Tbr1 (Abcam, ab31940, 1:1,000), to Akt (CST, 9272, 1:400 for immunoblot analysis), to Ndel1 (1:10,000) (kindly provided by K. Toyo-oka, Drexel University, Philadelphia) (61), to cleaved caspase-3 (CST, 9661, 1:1,000), to laminin (Sigma, L9393, 1:50), and to Foxp2 (Abcam, ab16046, 1:1,000); and rabbit monoclonal antibodies to Akt pT308 (CST, 2965, C31E5E, 1:300–1:500 for immunostaining), to phosphorylated Akt substrates (CST, 9614, 1:1,000 for immunoblot analysis and 1:500 for immunostaining), to Akt (pan) (CST, 4685, 11E7, 1:200 for immunostaining), to DLIC (Abcam, ab157468, 1:1,000), and to GSK3α (Upstate, 05–737, 1:500). Alexa-labeled secondary antibodies were obtained from Molecular Probes. Nuclei were stained with Hoechst 33342 (Molecular Probes) or TO-PRO3 (Invitrogen).

Retrovirus Production. Recombinant retroviruses encoding shRNAs or both GFP and the DsRed-pericentrin fusion protein were generated as described previously (57).

Primary Neuronal Culture and Immunocytofluorescence Analysis. The neocortex of E15.5 ICR or C57BL/6J mice was dissected in ice-cold DMEM–F12 (Sigma), transferred to artificial cerebrospinal fluid (aCSF: 124 mM NaCl, 5 mM KCl, 0.1 mM $CaCl_2$, 26 mM $NaHCO_3$, 1.3 mM $MgCl_2$, 10 mM glucose) containing 0.1% trypsin (Sigma), DNase I (0.1 mg/mL, Roche), and hyaluronidase (0.67 mg/mL, Sigma), and incubated at 37 °C for 10 min. After the addition of an equal volume of aCSF containing trypsin inhibitor (0.7 mg/mL, Sigma), the tissue was transferred to Neurobasal Medium (Gibco) and was dissociated mechanically into single cells. The dissociated cells were plated at a density of 4.0×10^5 to 5.0×10^5 cells/mL on poly-D-lysine–coated glass coverslips and were maintained in Neurobasal Medium supplemented with 1% GlutaMAX (Gibco) and 2% B27 (Invitrogen) for 3–4 DIV. For immunostaining, cells were fixed with 4% paraformaldehyde in PBS for 20 min at 37 °C, permeabilized with TBS/T [25 mM Tris·HCl (pH 7.5), 0.14 M NaCl, 0.1% Triton X-100] containing 2% donkey serum for 30 min at room temperature, incubated first overnight at 4 °C with primary antibodies in TBS/T containing 2% donkey serum and then for 30 min at room temperature with secondary antibodies in the same solution, and mounted in Mowiol (Calbiochem). Immunofluorescence for $p150^{glued}$ or Lis1 was quantified with the use of TCS-SP5 (Leica) software.

Immunoblot Analysis and Quantitative RT-PCR. Immunoblot analysis and quantitative RT-PCR were performed as described previously (58). The intensity of immunoblot bands was measured with an ImageQuant LAS 4000 instrument (GE Healthcare). The sense and antisense primers, respectively, were as follows: *Dync1i1*-cds, 5′-TTGAAGGAGCATCTGCCCTAAA-3′ and 5′-TCTCCAACATCGTAGATCCAAA-3′; *Dync1i1*-UTR, 5′-ATGATATGGTACAGGGCCAAA-3′ and 5′-AGCAGCAATGTTCTTGTAGT-3′; *Dync1li1*-cds, 5′-CATGAGAAGGAGATCATGGC-3′ and 5′-GTTGGAGGTTGCTTTGCTAA-3′; *Dync1li1*-UTR, 5′-CTGGCCTCAAACTCAGAAATC-3′ and 5′-TGGCAATGCAAACAGTTATTCTAC-3′; and *Actb*, 5′-AATAGTCATTCCAAGTATCCATGAAA-3′ and 5′-GCGACCATCCTCCTCTTAG-3′.

Microtubule Sedimentation. The forebrain of P0 mice was dissected, and one neocortical hemisphere was lysed in a solution containing 20 mM Tris·HCl (pH 7.5), 150 mM NaCl, 10 mM β-glycerophosphate, 5 mM EGTA, 1 mM $Na_4P_2O_7$, 5 mM NaF, 0.5% Triton X-100, 1 mM Na_3VO_4, 1 mM DTT, and protease inhibitors (1 mM phenylmethylsulfonyl fluoride, 1 μg/mL aprotinin, and 1 μg/mL leupeptin) to yield a total fraction. The other neocortical hemisphere was lysed in warm (37 °C) microtubule stabilization buffer [MSB: 100 mM Pipes-KOH (pH 6.8), 1 mM EGTA, 2 mM $MgCl_2$, 10% glycerol, 0.2% Triton X-100], and the lysate was centrifuged for 10 min at 20,400 × *g* and 35 °C. The resulting supernatant, representing the soluble fraction of tubulin, was removed and mixed with 5× Laemmli sample buffer; the pellet, representing the polymerized fraction of tubulin, was washed once with warm MSB and then was resuspended in 2× Laemmli sample buffer. Total, supernatant, and pellet fractions were subjected to immunoblot analysis with antibodies to α-tubulin and to GAPDH. The intensity of the insoluble and total α-tubulin bands was measured with an ImageQuant LAS 4000 instrument (GE Healthcare).

Purification of Microtubules and Associated MAPs. Microtubules and bound MAPs were purified from the brains of E19.5 control or $PDK1^{flox/flox}$;Nestin-Cre mice by temperature-dependent cycles of microtubule assembly and disassembly as described previously (62), with modifications. The brain was stripped of meninges and was homogenized manually in a 1-mL glass-Teflon homogenizer containing 0.7 mL/g of a buffer solution [100 mM Mes-NaOH (pH 6.8), 0.5 mM $MgCl_2$, and 1 mM EGTA] containing 0.2 mM GTP. The homogenate was centrifuged at 20,400 × *g* for 60 min at 4 °C. The resulting supernatant was mixed with a one-third volume of glycerol and 0.2 mM GTP and then was incubated for 20 min at 37 °C to allow assembly of microtubules. The microtubules were isolated by centrifugation at 20,400 × *g* for 45 min at 35 °C, and the supernatant was saved as the C1P fraction. The pellet was resuspended in the above buffer containing 0.2 mM GTP at 4 °C, homogenized gently with a glass-Teflon homogenizer at 4 °C, incubated on ice for 20 min to induce microtubule depolymerization, and centrifuged for 30 min at 20,400 × *g* and 4 °C. The resulting supernatant (the C1S fraction) was subjected to another cycle of microtubule assembly and disassembly as described above, yielding the C2P and C2S fractions. The various fractions obtained during the purification procedure were analyzed by electrophoresis (Fig. S4). The C2S fraction was examined by immunoblot analysis with the indicated antibodies (Fig. 7*B*).

Statistical Analysis. Data are presented as means ± SEM or SD and were analyzed with the two-tailed unpaired Student's *t* test or the Mann–Whitney test. A *P* value of <0.05 was considered statistically significant.

ACKNOWLEDGMENTS. We thank J. A. Cooper for critical reading of the manuscript; D. R. Alessi for PDK1 flox and GSK3 knock-in mice; R. Kageyama

for Nestin-Cre mice; A. K. Nave for Nex-Cre mice; D. R. Alessi, C. L. Cepko, T. Matsuda, T. Kitamura, F. Matsuzaki, R. Roth, F. Polleux, S. Munro, and K. Toyo-oka for reagents; M. Okajima and Y. Maeda for assistance; and members of the Y.G. laboratory for helpful discussions. This work was supported by Japan Society for the Promotion of Science Grant-in-Aid 23570249 (to Y.I.); a Grant-in-Aid for Scientific Research on Innovative Areas "Neural Diversity and Neocortical Organization" from the Ministry of Education, Culture, Sports, Science, and Technology (MEXT) of Japan; the Core Research for Evolutionary Science and Technology Program of the Japan Science and Technology Agency; and the Global Center of Excellence Program (Integrative Life Science Based on the Study of Biosignaling Mechanisms) of MEXT (Y.G.).

1. Rakic P (1972) Mode of cell migration to the superficial layers of fetal monkey neocortex. *J Comp Neurol* 145(1):61–83.
2. Angevine JB, Jr, Sidman RL (1961) Autoradiographic study of cell migration during histogenesis of cerebral cortex in the mouse. *Nature* 192:766–768.
3. Berry M, Rogers AW (1965) The migration of neuroblasts in the developing cerebral cortex. *J Anat* 99(Pt 4):691–709.
4. Rakic P (1974) Neurons in rhesus monkey visual cortex: Systematic relation between time of origin and eventual disposition. *Science* 183(4123):425–427.
5. Takahashi T, Goto T, Miyama S, Nowakowski RS, Caviness VS, Jr (1999) Sequence of neuron origin and neocortical laminar fate: Relation to cell cycle of origin in the developing murine cerebral wall. *J Neurosci* 19(23):10357–10371.
6. Gleeson JG, Walsh CA (2000) Neuronal migration disorders: From genetic diseases to developmental mechanisms. *Trends Neurosci* 23(8):352–359.
7. Itoh Y, Tyssowski K, Gotoh Y (2013) Transcriptional coupling of neuronal fate commitment and the onset of migration. *Curr Opin Neurobiol* 23(6):957–964.
8. Marín O, Valiente M, Ge X, Tsai LH (2010) Guiding neuronal cell migrations. *Cold Spring Harb Perspect Biol* 2(2):a001834.
9. Evsyukova I, Plestant C, Anton ES (2013) Integrative mechanisms of oriented neuronal migration in the developing brain. *Annu Rev Cell Dev Biol* 29:299–353.
10. Cooper JA (2013) Cell biology in neuroscience: Mechanisms of cell migration in the nervous system. *J Cell Biol* 202(5):725–734.
11. Tsai JW, Bremner KH, Vallee RB (2007) Dual subcellular roles for LIS1 and dynein in radial neuronal migration in live brain tissue. *Nat Neurosci* 10(8):970–979.
12. Solecki DJ, Model L, Gaetz J, Kapoor TM, Hatten ME (2004) Par6alpha signaling controls glial-guided neuronal migration. *Nat Neurosci* 7(11):1195–1203.
13. Akhmanova A, Steinmetz MO (2008) Tracking the ends: A dynamic protein network controls the fate of microtubule tips. *Nat Rev Mol Cell Biol* 9(4):309–322.
14. Desai A, Mitchison TJ (1997) Microtubule polymerization dynamics. *Annu Rev Cell Dev Biol* 13:83–117.
15. Williams MR, et al. (2000) The role of 3-phosphoinositide-dependent protein kinase 1 in activating AGC kinases defined in embryonic stem cells. *Curr Biol* 10(8):439–448.
16. Higuchi M, Onishi K, Kikuchi C, Gotoh Y (2008) Scaffolding function of PAK in the PDK1-Akt pathway. *Nat Cell Biol* 10(11):1356–1364.
17. Onishi K, Higuchi M, Asakura T, Masuyama N, Gotoh Y (2007) The PI3K-Akt pathway promotes microtubule stabilization in migrating fibroblasts. *Genes Cells* 12(4): 535–546.
18. Berzat A, Hall A (2010) Cellular responses to extracellular guidance cues. *EMBO J* 29(16):2734–2745.
19. Bock HH, et al. (2003) Phosphatidylinositol 3-kinase interacts with the adaptor protein Dab1 in response to Reelin signaling and is required for normal cortical lamination. *J Biol Chem* 278(40):38772–38779.
20. Konno D, Yoshimura S, Hori K, Maruoka H, Sobue K (2005) Involvement of the phosphatidylinositol 3-kinase/rac1 and cdc42 pathways in radial migration of cortical neurons. *J Biol Chem* 280(6):5082–5088.
21. Dummler B, Hemmings BA (2007) Physiological roles of PKB/Akt isoforms in development and disease. *Biochem Soc Trans* 35(Pt 2):231–235.
22. Franke TF (2008) PI3K/Akt: Getting it right matters. *Oncogene* 27(50):6473–6488.
23. Lawlor MA, et al. (2002) Essential role of PDK1 in regulating cell size and development in mice. *EMBO J* 21(14):3728–3738.
24. Isaka F, et al. (1999) Ectopic expression of the bHLH gene Math1 disturbs neural development. *Eur J Neurosci* 11(7):2582–2588.
25. Oishi K, et al. (2009) Selective induction of neocortical GABAergic neurons by the PDK1-Akt pathway through activation of Mash1. *Proc Natl Acad Sci USA* 106(31): 13064–13069.
26. Kitazawa A, et al. (2014) Hippocampal pyramidal neurons switch from a multipolar migration mode to a novel "climbing" migration mode during development. *J Neurosci* 34(4):1115–1126.
27. Goebbels S, et al. (2006) Genetic targeting of principal neurons in neocortex and hippocampus of NEX-Cre mice. *Genesis* 44(12):611–621.
28. Bartholomä A, Nave KA (1994) NEX-1: A novel brain-specific helix-loop-helix protein with autoregulation and sustained expression in mature cortical neurons. *Mech Dev* 48(3):217–228.
29. Pearce LR, Komander D, Alessi DR (2010) The nuts and bolts of AGC protein kinases. *Nat Rev Mol Cell Biol* 11(1):9–22.
30. Kohn AD, Summers SA, Birnbaum MJ, Roth RA (1996) Expression of a constitutively active Akt Ser/Thr kinase in 3T3-L1 adipocytes stimulates glucose uptake and glucose transporter 4 translocation. *J Biol Chem* 271(49):31372–31378.
31. Kato TM, Kawaguchi A, Kosodo Y, Niwa H, Matsuzaki F (2010) Lunatic fringe potentiates Notch signaling in the developing brain. *Mol Cell Neurosci* 45(1):12–25.
32. Morgan-Smith M, Wu Y, Zhu X, Pringle J, Snider WD (2014) GSK-3 signaling in developing cortical neurons is essential for radial migration and dendritic orientation. *eLife* 3:e02663.
33. McManus EJ, et al. (2005) Role that phosphorylation of GSK3 plays in insulin and Wnt signalling defined by knockin analysis. *EMBO J* 24(8):1571–1583.
34. Gillingham AK, Munro S (2000) The PACT domain, a conserved centrosomal targeting motif in the coiled-coil proteins AKAP450 and pericentrin. *EMBO Rep* 1(6):524–529.
35. Kardon JR, Vale RD (2009) Regulators of the cytoplasmic dynein motor. *Nat Rev Mol Cell Biol* 10(12):854–865.
36. Zhang J, et al. (2013) AKT activation by N-cadherin regulates beta-catenin signaling and neuronal differentiation during cortical development. *Neural Dev* 8:7.
37. Ka M, Condorelli G, Woodgett JR, Kim WY (2014) mTOR regulates brain morphogenesis by mediating GSK3 signaling. *Development* 141(21):4076–4086.
38. Jossin Y, Goffinet AM (2007) Reelin signals through phosphatidylinositol 3-kinase and Akt to control cortical development and through mTor to regulate dendritic growth. *Mol Cell Biol* 27(20):7113–7124.
39. Polleux F, Whitford KL, Dijkhuizen PA, Vitalis T, Ghosh A (2002) Control of cortical interneuron migration by neurotrophins and PI3-kinase signaling. *Development* 129(13):3147–3160.
40. Nadarajah B, Brunstrom JE, Grutzendler J, Wong RO, Pearlman AL (2001) Two modes of radial migration in early development of the cerebral cortex. *Nat Neurosci* 4(2): 143–150.
41. Miura H, Matsuda M, Aoki K (2014) Development of a FRET biosensor with high specificity for Akt. *Cell Struct Funct* 39(1):9–20.
42. Jossin Y, Cooper JA (2011) Reelin, Rap1 and N-cadherin orient the migration of multipolar neurons in the developing neocortex. *Nat Neurosci* 14(6):697–703.
43. Medina DL, et al. (2004) TrkB regulates neocortex formation through the Shc/PLCgamma-mediated control of neuronal migration. *EMBO J* 23(19):3803–3814.
44. Ip JP, et al. (2011) α2-chimaerin controls neuronal migration and functioning of the cerebral cortex through CRMP-2. *Nat Neurosci* 15(1):39–47.
45. Osborne JK, et al. (2013) NeuroD1 regulates survival and migration of neuroendocrine lung carcinomas via signaling molecules TrkB and NCAM. *Proc Natl Acad Sci USA* 110(16):6524–6529.
46. Chen ZL, Haegeli V, Yu H, Strickland S (2009) Cortical deficiency of laminin gamma1 impairs the AKT/GSK-3beta signaling pathway and leads to defects in neurite outgrowth and neuronal migration. *Dev Biol* 327(1):158–168.
47. Kawauchi T, et al. (2010) Rab GTPases-dependent endocytic pathways regulate neuronal migration and maturation through N-cadherin trafficking. *Neuron* 67(4): 588–602.
48. Buttrick GJ, et al. (2008) Akt regulates centrosome migration and spindle orientation in the early Drosophila melanogaster embryo. *J Cell Biol* 180(3):537–548.
49. Duellberg C, et al. (2014) Reconstitution of a hierarchical +TIP interaction network controlling microtubule end tracking of dynein. *Nat Cell Biol* 16(8):804–811.
50. Zhou T, Zimmerman W, Liu X, Erikson RL (2006) A mammalian NudC-like protein essential for dynein stability and cell viability. *Proc Natl Acad Sci USA* 103(24): 9039–9044.
51. Zhou J, Parada LF (2012) PTEN signaling in autism spectrum disorders. *Curr Opin Neurobiol* 22(5):873–879.
52. Poduri A, Evrony GD, Cai X, Walsh CA (2013) Somatic mutation, genomic variation, and neurological disease. *Science* 341(6141):1237758.
53. Emamian ES (2012) AKT/GSK3 signaling pathway and schizophrenia. *Front Mol Neurosci* 5:33.
54. Higuchi M, Masuyama N, Fukui Y, Suzuki A, Gotoh Y (2001) Akt mediates Rac/Cdc42-regulated cell motility in growth factor-stimulated cells and in invasive PTEN knockout cells. *Curr Biol* 11(24):1958–1962.
55. Matsuda T, Cepko CL (2004) Electroporation and RNA interference in the rodent retina in vivo and in vitro. *Proc Natl Acad Sci USA* 101(1):16–22.
56. Morita S, Kojima T, Kitamura T (2000) Plat-E: An efficient and stable system for transient packaging of retroviruses. *Gene Ther* 7(12):1063–1066.
57. Itoh Y, Masuyama N, Nakayama K, Nakayama KI, Gotoh Y (2007) The cyclin-dependent kinase inhibitors p57 and p27 regulate neuronal migration in the developing mouse neocortex. *J Biol Chem* 282(1):390–396.
58. Itoh Y, et al. (2013) Scratch regulates neuronal migration onset via an epithelial-mesenchymal transition-like mechanism. *Nat Neurosci* 16(4):416–425.
59. Tabata H, Nakajima K (2001) Efficient in utero gene transfer system to the developing mouse brain using electroporation: Visualization of neuronal migration in the developing cortex. *Neuroscience* 103(4):865–872.
60. Ogawa M, et al. (1995) The reeler gene-associated antigen on Cajal-Retzius neurons is a crucial molecule for laminar organization of cortical neurons. *Neuron* 14(5): 899–912.
61. Toyo-oka K, et al. (2003) 14-3-3epsilon is important for neuronal migration by binding to NUDEL: A molecular explanation for Miller-Dieker syndrome. *Nat Genet* 34(3): 274–285.
62. Karr TL, White HD, Purich DL (1979) Characterization of brain microtubule proteins prepared by selective removal of mitochondrial and synaptosomal components. *J Biol Chem* 254(13):6107–6111.